Atmos. Meas. Tech. Discuss., 6, 1979–2008, 2013
www.atmos-meas-tech-discuss.net/6/1979/2013/
doi:10.5194/amtd-6-1979-2013

Atmospheric Measurement Techniques Discussions

Systematic residual ionospheric errors in radio occultation data and a potential way to minimize them

J. Danzer[1,2], **B. Scherllin-Pirscher**[1,2], **and U. Foelsche**[1,2]

[1]Wegener Center for Climate and Global Change (WEGC), University of Graz, Graz, Austria
[2]Institute for Geophysics, Astrophysics, and Meteorology/Institute of Physics (IGAM/IP), University of Graz, Graz, Austria

Received: 14 December 2012 – Accepted: 8 February 2013 – Published: 20 February 2013

Correspondence to: J. Danzer (julia.danzer@uni-graz.at)

Published by Copernicus Publications on behalf of the European Geosciences Union.

Abstract

Radio Occultation (RO) sensing is used to probe the Earth's atmosphere in order to obtain information about its physical properties. With a main interest in the parameters of the neutral atmosphere, there is the need to perform a correction of the ionospheric contribution to the bending angle. Since this correction is an approximation to first order, there exists an ionospheric residual, which can be expected to be larger when the ionization is high (day versus night, high versus low solar activity). The ionospheric residual systematically affects the accuracy of the atmospheric parameters at low altitudes, at high altitudes (above 25 km to 30 km) it even is an important error source. In climate applications this could lead to a time dependent bias which induces wrong trends in atmospheric parameters at high altitudes. The first goal of our work was to study and characterize this systematic residual error. In a second step we developed a simple correction method, based purely on observational data, to reduce this residual for large ensembles of RO profiles. In order to tackle this problem we analyzed the bending angle bias of CHAMP and COSMIC RO data from 2001 to 2011. We could observe that the night time bending angle bias stays constant over the whole period of 11 yr, while the day time bias increases from low to high solar activity. As a result, the difference between night and day time bias increases from about −0.05 µrad to −0.4 µrad. This behavior paves the way to correct the solar cycle dependent bias of day time RO profiles. In order to test the newly developed correction method we performed a simulation study, which allowed to separate the influence of the ionosphere and the neutral atmosphere. Also in the simulated data we observed a similar increase in the bias in times from low to high solar activity. In this model world we performed the climatological ionospheric correction of the bending angle data, by using the bending angle bias characteristics of a solar cycle as a correction factor. After the climatological ionospheric correction the bias of the simulated data improved significantly, not only in the bending angle but also in the retrieved temperature profiles.

AMTD
6, 1979–2008, 2013

1 Introduction and motivation

The Radio Occultation (RO) method (Melbourne et al., 1994; Kursinski et al., 1997; Hajj et al., 2002) is an active satellite to satellite limb sounding technique. Measurements are performed when a Global Positioning System (GPS) satellite transmits an electromagnetic signal, which is recorded at a Low Earth Orbit (LEO) satellite. The path of the transmitted electromagnetic signal changes when passing through the ionosphere and neutral atmosphere. Consequential the received total terrestrial phase delay consists of a neutral atmospheric phase delay and an ionospheric phase delay. However, it is possible to remove the ionospheric contribution to first order by applying an ionospheric correction (e.g. Spilker, 1980; Vorobev and Krasilnikova, 1994; Ladreiter and Kirchengast, 1996; Syndergaard, 2000; Sokolovskiy et al., 2009) in order to obtain phase delay or bending angle profiles of the neutral atmosphere. Nevertheless, higher order ionospheric errors remain.

The received signal's phase delay enables to retrieve near vertical profiles of atmospheric parameters, with highest accuracy in the upper troposphere and lower stratosphere (UTLS). It provides information about bending angle and radio refractive index of the Earth's atmosphere. The atmospheric parameters are used for research areas such as numerical weather prediction, atmospheric research, and climate studies. If the main interest is in the characteristics of the neutral atmosphere, there is a need to study the ionospheric residual, which systematically affects the atmospheric parameters, more thoroughly (e.g. Kursinski et al., 1997; Gobiet and Kirchengast, 2004; Mannucci et al., 2011).

GPS satellites transmit electromagnetic signals on two carrier frequencies in the L-band (f_1 = 1575.42 MHz and f_2 = 1227.60 MHz). In RO measurements the primary observables are the phase delays of those two frequencies. From the phase delays bending angle profiles can be derived, which are related to refractive index (n) profiles via an inverse Abel-transform (Fjeldbo et al., 1971). Using the relation $N = (n - 1) \cdot 10^6$ the refractivity N is obtained, which can be expressed as a function of height z.

AMTD
6, 1979–2008, 2013

To first order the refractivity can be written as (Smith and Weintraub, 1953; Kursinski et al., 1997)

$$N(z) = 77.6\frac{p(z)}{T(z)} + 3.73 \times 10^5 \frac{e(z)}{T^2(z)} - 4.03 \times 10^7 \frac{N_e(z)}{f_k^2} + 1.4W(z), \quad (1)$$

with p being the atmospheric pressure (in hPa), T the temperature (in K), e is the partial pressure of water vapor (in hPa), N_e is the electron density (in electrons per m^3), f_k is the transmitter frequency (1,2) (in Hz) and W is the mass of condensed water in the atmosphere (in g per m^3). The four contributions are usually referred to as dry atmosphere, moist atmosphere, ionosphere, and atmospheric scattering from liquid water. The liquid water term is very small and generally negligible. The ionospheric contribution is given to first order and will be corrected at bending angle level. If also the moist contribution is neglected it yields dry atmospheric parameters. Combining the refractivity equation with the equation of state and the hydrostatic equation leads to atmospheric parameters such as dry density, dry pressure, and dry temperature.

In general the ionospheric refractivity is described by the Appelton-Hartree formula, see, e.g. Budden (1985):

$$N_k^{IO} \approx \left[-C\frac{N_e}{f_k^2} - K\frac{B_{par}N_e}{f_k^3} + ... \right] \times 10^6, \quad (2)$$

where the index k denotes again the transmitter signal (1,2) and C is the constant of Eq. (1) ($C = 40.3\,m^3\,s^{-2}$). The value of the constant of the second order term is $K = 1.13 \times 10^{-12}\,m^3\,T^{-1}\,s^{-3}$ and B_{par} is the absolute value of the Earth's magnetic field parallel to the wave propagation [T].

In the analysis of RO data, terms higher than second order of the ionospheric refractivity (N_k^{IO}) are generally neglected (Hardy et al., 1994; Melbourne et al., 1994), resulting in a second order approximation (Bassiri and Hajj, 1993). The second order term is proportional to the inverse cube of the carrier frequency, and shows almost no

AMTD
6, 1979–2008, 2013

influence to a changing solar activity. The usual approach is to perform a first order ionospheric correction, as discussed below, but there are also attempts for a reduction of the ionospheric residual by taking the second order term into account (e.g. Kedar et al., 2003; Petrie et al., 2011; Vergados and Pagiatakis, 2011). A disadvantage of the second order approximation is that it is model dependent and requires further informations, such as, the electron density in the vicinity of the ray path or the geomagnetic field.

The refractive properties of the atmosphere (combining neutral atmospheric and ionospheric refractivity) lead to delays of the wave's phase. Hence the optical path L_k of an electromagnetic wave ($k = 1,2$) is defined as:

$$L_k = \int_{S_k} n \, \mathrm{d}s = \int_{S_k} 1 + \frac{N_k^{\mathrm{IO}} + N^{\mathrm{NA}}}{10^6} \, \mathrm{d}s, \tag{3}$$

where the integral is along the ray path S_k. Equation (3) can be rewritten as an integral over the ionospheric refractivity N_k^{IO} and neutral atmospheric refractivity N^{NA}. While the neutral atmosphere is not a dispersive medium, the ionosphere is, and hence influences the two carrier frequencies in a different way. Due to this dispersive nature the frequencies f_1 and f_2 experience different phase delays and result in unequal optical paths L_1 and L_2.

However, a linear combination of the two signals leads to a correction term to first order (e.g. Spilker, 1980):

$$L_{\mathrm{C}}(t) = \frac{f_1^2 L_1(t) - f_2^2 L_2(t)}{f_1^2 - f_2^2}, \tag{4}$$

where $L_{\mathrm{C}}(t)$ is the ionosphere corrected optical path [m], t is time [s] and $L_{1,2}$ are the measured optical paths [m].

Equation (4) is the so-called traditional linear correction of phase delays, which contains two important simplifications. First, it neglects higher order terms, and second, it

AMTD
6, 1979–2008, 2013

assumes that the two signals are traveling along the same paths, which is not fulfilled due to the dispersive nature of the ionosphere. This suggests an ionospheric residual ("dispersion" residual) especially during day time, and times of high solar activity (Syndergaard, 2000). On the other hand the advantage of the correction is that it does not exploit spherical symmetry, which is highly violated due to the variable ionosphere.

It is also possible to write an ionospheric correction as a correction of bending angels α (Vorobev and Krasilnikova, 1994), which has the advantage that it does not assume identical ray paths. It is applied at same impact parameters a:

$$\alpha_C(a) = \frac{f_1^2 \alpha_1(a) - f_2^2 \alpha_2(a)}{f_1^2 - f_2^2}, \quad (5)$$

with α_C being the ionosphere corrected bending angle and $\alpha_{1,2}$ being the bending angles of the signals. (A modified version of Eq. (5), described by Hocke et al., 2003, with the aim of more stability and reduction of noise-amplification, is applied at WEGC.)

Nonetheless, Eqs. (4) and (5) are still approximations, which neglect higher order terms and do not address small scale structures of the ionosphere. The ionospheric residual systematically affects the accuracy of the data at low as well as at high altitudes, increasing with altitude (see Sect. 4.2). The error is carried through the retrieval of the atmospheric parameters. This leads to the conclusion that residual ionospheric errors in the RO data must be studied more thoroughly. Research related to that has been performed by Rocken et al. (2008, 2009) and Schreiner et al. (2011). Their studies show that the effect of the residual error is smallest in the bending angle data. At 60 km altitude they found day time bending angle errors of about −0.02 µrad in 2007 (solar minimum) and of about −0.1 µrad in 2002 (solar maximum). The ionosphere induced errors are enhanced when retrieving refractivity N and temperature T with up to 0.045 % (0.1 K) at 20 km altitude and 0.2 % (0.5 K) at 30 km altitude, during day time. The error decreases during the night time to 0.0006 % (0.002 K) at 20 km and 0.004 % (0.01 K) at 30 km altitude (Rocken et al., 2008).

AMTD
6, 1979–2008, 2013

Extending this work we focused on residuals caused by the change of ionization from day and night and from low to high solar activity. Therefore we studied systematic residual errors for a period of 11 yr (approximately one solar cycle) with the aim of providing an estimate of its time dependent magnitude (Sect. 3.1). Furthermore we performed a model study with simulated data, where we separately analyzed the influence of the ionosphere and neutral atmosphere (Sect. 3.2). In a second step we applied a climatological ionospheric correction (Sect. 4) which reduces the systematic residual ionospheric error.

In our approach we averaged over many RO profiles within a latitude zone and study their residual error for a solar cycle. This delivers a correction factor dependent on solar radiation, which is applied at bending angle level. The advantage is that it is a simple, model independent approach, which only uses observational RO data for the correction. The goal is not to reduce the residual error for a single profile, but to correct the ionospheric residual of large ensembles of RO profiles, which are used for climatological studies.

2 Data sets and method

2.1 Satellite data

In order to detect the residual ionospheric error, we investigated the bending angle bias (see Sect. 2.3) over a time period from 2001 to 2011, using CHAMP (CHAllenging Minisatellite Payload) and Formosat-3/COSMIC (Constellation Observing System for Meteorology, Ionosphere and Climate) RO data, comparing WEGC Occultation Processing System version 5.4 (OPSv5.4) (Steiner et al., 2009; Pirscher, 2010) and UCAR (University Corporation for Atmospheric Research) data processings (Kuo et al., 2004; Ho et al., 2009). CHAMP data have been available from May 2001 to September 2008 and COSMIC were used from August 2006 to September 2011. The UCAR/CDAAC (COSMIC Data Analysis and Archive Center) retrieval (version 2010.2640) starts with

AMTD
6, 1979–2008, 2013

raw GPS amplitude and phase measurements as well as raw GPS and LEO orbit tracking data. The WEGC OPSv5.4 retrieval starts with excess phase profiles and precise orbit information, provided by UCAR/CDAAC.

2.2 Simulated data

With the EGOPS software (End-to-End Generic Occultation Performance and Processing System) version 5.5 (Fritzer et al., 2009) we performed an End-to-End simulation study similar to Foelsche et al. (2008). We simulated day time events (12:00, local time) and night time events (02:00, local time) for the years 2001 to 2011 via ray tracing through ionospheric and neutral atmospheric fields. The resulting phase data were used as input for standard RO retrieval of atmospheric parameters from bending angle to dry temperature. Since we focused on the separation of ionospheric errors we did not superimpose observational errors.

We performed two different studies. In the first study we always employed the same atmosphere, using operational analysis fields provided by ECMWF (European Center for Medium-Range Weather Forecasts) for all simulations, and only varied the ionosphere for each profile. The ECMWF field used in this analysis is from the day 1 January 2007 with T42L91 resolution. The horizontal resolution T42 corresponds to the resolution of RO data (~ 300 km), with data available at 91 vertical levels (L91). The ionosphere was simulated with the NeUoG model (with Ne being the electron density and UoG means University of Graz (Leitinger et al., 1995, 1997)), which is driven by the $F_{10.7}$ index as an indicator for the solar activity. The $F_{10.7}$ index is based on the solar radio flux at a wavelength of 10.7 cm. We downloaded daily $F_{10.7}$ data from the website of the National Oceanic and Atmospheric Administration, NOAA (ftp://ftp.ngdc.noaa.gov/STP/SOLAR_DATA/SOLAR_RADIO/FLUX/Penticton_Observed/daily/DAILYPLT.OBS, 2012) and calculated monthly mean values as a representative for typical solar activity, see Fig. 1. The NeUoG model provides a global 3-D electron density distribution depending on local time, season, and solar activity. As an example Fig. 2 shows typical day and night ionospheric conditions

AMTD
6, 1979–2008, 2013

simulated with NeUoG. The plots show the electron density distribution N_e as a function of height and latitude. In this particular example the solar activity is characterized by $F_{10.7}$ = 140 sfu, for January at longitude 0°. As expected, the ionization level in Fig. 2 is clearly increased during day time (bottom panel) compared to the night time (top panel). Furthermore there is a dependance of the ionization on the latitude and altitude. At night there is a maximum around 3° N (top panel), while during the day there are two maxima around 10° S and 18° N, at an altitude of 400 km (bottom panel), illustrating the equatorial anomaly (the maximum of N_e is not at the equator, but within ±20° latitude of the magnetic equator).

In our simulations we focused on the latitude band 20° S to 20° N and simulated events taking place in all Januaries from 2001 to 2011 at latitudes 0°, 5° S, 5° N, 10° S, 10° N and at longitudes 0°, 60° E, 60° W, 120° E, 120° W, 180° E. This leads to altogether 60 simulated occultation events per year and 660 events for a period of 11 yr. This is not a representative statistics, but sufficient to study the two main questions:

1. What are the bias characteristics of the ionosphere alone in the years 2001 to 2011?

2. Does, as a first test, a climatological ionospheric correction work on the simulated data?

Furthermore we simulated occultation events based on past realistic atmospheric fields, where the electromagnetic signal gets occulted only by the neutral atmosphere, i.e. the ionospheric part was ignored in that simulation. We analyzed the following questions:

1. How big is the contribution of the neutral atmosphere in the altitude domain where the ionospheric residual is determined?

2. Does this contribution of the neutral atmosphere vary during a solar cycle?

For that study we simulated two profiles per month (one day and one night profile) for the years 2001 to 2009 at longitude and latitude 0°, which makes alltogether 216

AMTD
6, 1979–2008, 2013

profiles. In order to study the contribution of the neutral atmosphere we used the ECMWF analysis field of the first day of each month at 00:00 UTC and 12:00 UTC, respectively.

2.3 Determination of the ionospheric residual

The residual ionospheric error was studied by analyzing the bending angle bias. At WEGC the bias is obtained by comparing the ionosphere corrected bending angle profile α with the co-located MSIS (Mass Spectrometer and Incoherent Scatter Radar) bending angle profile between 65 km and 80 km impact height (which is defined as the impact parameter minus the local radius of curvature).

$$\text{bias} = \frac{1}{l}\sum_{i=1}^{l}(\alpha_{\text{RO}} - \alpha_{\text{MSIS}})_i, \tag{6}$$

where $i = 1$ corresponds to the first altitude level above 65 km and l is the last level below 80 km. We studied the day and night time bias for three different latitude zones: 60° S to 20° S, 20° S to 20° N and 20° N to 60° N. As night time events we regarded RO events taking place from 02:00 to 06:00 in the morning, for the day time bias we considered occultation events between 11:00 and 15:00, local time (LT). The time frames for the night time and day time events have been chosen to allow comparisons with results by Rocken et al. (2008, 2009); Schreiner et al. (2011) who picked the same time frames.

At UCAR the bending angle bias is calculated in a similar way, but in the altitude range of 60 km to 80 km. As a reference climatology they use the NCAR (National Center for Atmospheric Research) climatology (Randel et al., 2002). Hence, the absolute bias values are different for WEGC and UCAR data.

We calculated the median bias of all profiles which pass WEGC quality control, within three months for CHAMP data, and within one month for COSMIC data. This leads to about 600 events (CHAMP) and about 4000 events (COSMIC), per latitude zone and

AMTD
6, 1979–2008, 2013

day or night time event frame. CHAMP is a single satellite which performs only setting events, i.e. the satellite scans the atmosphere from top to bottom. However, COSMIC is a six satellite constellation, which measures setting as well as rising events (scanning of the atmosphere from bottom to top), leading to considerably fewer CHAMP RO profiles. Therefore we averaged CHAMP data over three months and took the central month as a representative for this month, e.g. the median bias over the period March-April-May represents April.

3 Results and discussion of the ionospheric residual

3.1 Satellite data results

In Fig. 3 we show the day (11:00–15:00 LT) and night (02:00–06:00 LT) time bending angle bias for 10 yr (WEGC) and 11 yr (UCAR), for three latitude zones (see Sect. 2.3). Until July 2006 we used CHAMP data for the analysis, afterwards we continued with COSMIC data, since the number of RO profiles is higher. The combination of CHAMP and COSMIC data is feasible, since the bias characteristics of both data sets are extremely similar (see Foelsche et al., 2011, and an explicit discussion below). In this 10 to 11 yr time frame the solar cycle has a maximum in the years 2001 and 2002, and a minimum in the years 2007 to 2009 (see Fig. 1). We know that the MSIS climatology is not the "truth", but it serves as a good reference climatology. The negative sign of the bias is consistent with the assumption of an ionospheric origin (Sokolovskiy et al., 2009). The time series in Fig. 3 illustrates three main effects:

1. The negative bending angle bias is larger during day time than during night time (diurnal cycle).

2. The day time bending angle bias increases with solar activity, while the night time bias remains nearly constant (solar cycle).

AMTD
6, 1979–2008, 2013

3. Within a year the day time and night time bending angle biases show maxima in the summer months in WEGC data (seasonal cycle).

The diurnal cycle can be explained by the increase of ionization from night to day. Also the second effect reflects the change of ionization, caused by the solar cycle. Indeed we find that in the years of high solar activity the day time bending angle bias increases in all three latitude zones. In the solar minimum years Fig. 3 shows that the WEGC as well as the UCAR bending angle data sets approach a more or less constant value. Furthermore the WEGC data sets show a seasonal dependance, reflected in the yearly peaks of the day time and night time bending angle bias. The seasonal maxima depend on the latitude zone. In the extra tropics maxima occur in summer: in the Northern Hemisphere in June and July (top panel of Fig. 3) and in the Southern Hemisphere in December and January (bottom panel of Fig. 3). Only the tropical zone (central panel of Fig. 3) shows no definite maxima. Finally, in the comparison of the WEGC and UCAR processed data sets we observe that the absolute bias values differ from each other. This is due to the different altitude ranges (see Sect. 2.3) and the different reference climatologies, which are used in the calculation of the bending angle biases.

Nevertheless, the difference between day time and night time bending angle bias should be the same (ΔBias = Day Bias – Night Bias) for the two data sets, if it correctly reflects the changing solar activity. This is confirmed by the results shown in Fig. 4, by comparing WEGC data (green line) and UCAR processed data (blue line). The two data sets display a very similar temporal evolution. This characteristic can be found in all three latitude zones. Furthermore, the bias difference in all three zones approaches a constant value in 2007, which could indicate that the seasonal cycle in Fig. 3 for WEGC data is due to the reference climatology used. The similar behavior of two data sets obtained with different processing methods strengthens the conclusion that the observed bias difference between day and night is indeed caused by solar activity. This bending angle bias difference will therefore be used as a solar cycle dependent correction factor for the bending angle data (see Sect. 4.1).

AMTD
6, 1979–2008, 2013

In Fig. 5 we discuss the potential impact of mixing CHAMP and COSMIC satellite data (processed at WEGC) in a 10 yr bending angle bias time series in the latitude zone 20° S to 20° N. The top plot of Fig. 5 shows again the day time and night time bending angle bias characteristics, while the bottom plot shows the bending angle bias difference Δ Bias. In contrast to the previous plots we now compare the complete available WEGC data sets of CHAMP and COSMIC. CHAMP data are available from May 2001 to September 2008 and COSMIC data from August 2006 to December 2010. We find that the data of the two satellites are in good agreement in the overlapping period from August 2006 to September 2008. Confirming the results of Foelsche et al. (2011) we find very similar bias results for the two satellites. Small deviations have to be expected, since we computed monthly averages for COSMIC data, while we calculated three month averages for CHAMP, due to the smaller number of profiles – which also explains the higher variability in the CHAMP record.

Finally, we conclude that Figs. 3 and 4 clearly demonstrate that despite of the ionospheric correction, which has been applied to the bending angle data (see Eq. 5), an ionospheric residual exists, which results in a negative bending angle bias. The ionospheric correction does not catch the complete change of ionization during a solar cycle. In the next subsection this problem will be addressed with simulated data.

3.2 Simulation results

In Fig. 6 we show the mean bending angle bias for simulated profiles in the tropical band. At each latitude (0°, 5° S, 5° N, 10° S, 10° N) we simulated profiles at longitudes 0°, 60° E, 60° W, 120° E, 120° W, 180° E. We studied the day time (12:00 LT) and night time (02:00 LT) bending angle bias for the years 2001 to 2011. Thereby we always used the same ECMWF atmosphere field for all profiles and varied only the solar activity according to Fig. 1.

The top panel of Fig. 6 shows the results of the mean day time and night time bending angle bias characteristics. For each data point we averaged over 30 profiles. Also in the simulated case we can observe that the night time bias stays more or less constant

AMTD
6, 1979–2008, 2013

during a solar cycle (blue line), while the day time bending angle bias shows a response to the modifying solar radiation (orange line). The negative night time bias fluctuates around a mean value of about −0.1 µrad, while the day time bias changes from about −0.27 µrad to about −0.15 µrad from high to low solar activity.

Following the same approach as for observational data in Fig. 4, we show in the bottom panel of Fig. 6 the bending angle bias difference between day and night (Δ Bias, red line). For comparison, we show the WEGC processed observational data in the same latitude zone (20° S to 20° N, green line). One can see that the mean value of the simulated data nicely fits the observational bending angle bias difference. We do not expect full coincidence between the absolute values of the bending angle bias difference of observational and the simulated RO data (the latter being a characteristicum of NeUoG model used), but it is encouraging to see that the simulated results show a similar behavior: the stable night time bias and the solar cycle dependent day time bias could be confirmed in the model simulation.

Finally, the bottom panel of Fig. 6 also contains the simulation results of the neutral atmosphere (magenta line) at latitude and longitude 0° (see Sect. 2.2), using ECMWF operational analysis fields from the years 2001 to 2009. We simulated the pure effect of the neutral atmosphere without ionosphere, because we wanted to provide an estimate of the contribution of the neutral atmosphere to the bending angle bias between 65 km and 80 km. Furthermore we wanted to study if this contribution shows a dependance on the solar cycle. We observed that the contribution of the neutral atmosphere stays stable during a solar cycle, resulting in a Δ Bias that fluctuates around a mean value of −0.006 µrad. At least in the ECMWF analysis fields, the contribution of the neutral atmosphere is small and almost constant.

AMTD
6, 1979–2008, 2013

4 Climatological ionospheric correction

4.1 A simple bending angle correction factor

Now we want to introduce an idea for a simple correction of the ionospheric residual, which has been identified in Sect. 3.

Based on the results of Sect. 3 we identify the difference between day and night time bias as a good indicator for the ionospheric residual. Since the residual depends on latitude and on the phase of the solar cycle, we propose a correction of the day time profiles, which is applied at bending angle level, as follows:

$$\alpha_{C'_{i,\mathrm{SL}}} = \alpha_{C_{i,\mathrm{SL}}} - (\Delta\mathrm{Bias}_{\mathrm{SL}} - \Delta\mathrm{Bias}_{\mathrm{Neut}_{\mathrm{SL}}}), \quad (7)$$

where α_C is the original bending angle, after standard first order ionospheric correction (see Eq. 5), $\alpha_{C'}$ is the new bending angle after the additional *climatological* ionospheric correction, ΔBias is the bending angle difference between day and night and $\Delta\mathrm{Bias}_{\mathrm{Neut}}$ is the small contribution of the neutral atmosphere in the altitude range where the bias is determined, which should not be corrected. The subscript i indicates that the bending angles α_C and $\alpha_{C'}$ are vectors depending on the impact height. The subscript L denotes the latitude zone in which the occultation event takes place. In our studies we distinguished three different latitude zones. Finally, the subscript S stands for the point in time of the solar cycle. Hence, we subtract a correction factor from a day time bending angle profile, which magnitude depends on the phase of the solar cycle and the latitude zone in which the occultation event takes place. Furthermore we subtract the small neutral atmospheric contribution from the correction factor. A first test of this approach is presented in the next section.

4.2 Model results on the reduction of the systematic residual ionospheric error

As a next step we used the simulated profiles to perform a first test of the newly introduced climatological ionospheric correction. We tested the performance of the

AMTD
6, 1979–2008, 2013

correction over a solar cycle on two different geographic locations (at latitude 0° and 5° S, both at longitude 0°).

The correction factor we used is the mean bending angle bias difference (Δ Bias) of all simulated profiles (red line of bottom panel of Fig. 6). From this mean bending angle bias difference we subtracted the contribution of the neutral atmosphere ($\Delta\text{Bias}_{\text{Neut}}$). Since we used the same ECMWF analysis field (1 January 2007) for every profile simulated with ionosphere, in our special case we always subtracted the same neutral atmospheric contribution ($\Delta\text{Bias}_{\text{Neut}}$) from our bending angle bias difference ($\Delta\,\text{Bias}_{\text{SL}}$). For this particular day $\Delta\text{Bias}_{\text{Neut}}$ amounts to a value of about 1.8×10^{-8} rad. The next step is to correct the day time bending angle α_{C} with this mean bending angle bias difference according to Eq. (7), i.e. the whole profile is shifted by the same correction factor. As explained in Sect. 4.1, the magnitude of the correction factor depends on the latitude zone and the phase of the solar cycle. This leads to a larger correction factor in times of high solar activity and a smaller factor in times of low solar activity.

Figure 7 illustrates the day time to night time bending angle bias difference before (blue solid lines) and after (green dashed lines) the climatological ionospheric correction. The top plot shows the bias difference for the latitude 0°, the bottom plot for 5° S. As expected, the 0° and 5° S bending angle profiles show a smaller day time to night time bending angle bias difference after the correction (see dashed lines of Fig. 7). There is still a dependance of the bias difference on the solar radiation, but the residual clearly reduced.

Next we studied if this reduction of the bending angle bias also results in a bias reduction of the derived parameter dry temperature. The results for 0° and 5° S are very similar, Fig. 8 shows those for 0° as a representative example. We cut the profiles below 10 km altitude, since here the difference between dry and physical temperature becomes important, which is not the focus of this study. In Fig. 8 we show the day time (12:00 LT) January dry temperature profiles for the years 2001 to 2011. Besides being an important parameter for climate research, temperature profiles are of special interest, since they illustrate how the ionospheric error is carried through the retrieval

AMTD
6, 1979–2008, 2013

(Sect. 2.2). The top row shows dry temperature profiles up to 80 km altitude and the "true" ECMWF temperature profile (dashed red line) is plotted, which has been used as input for the simulation. The bottom row of the figure displays the temperature difference of each profile to this ECMWF profile, in the altitude range up to 35 km, where RO profiles are frequently used for climatological studies. The left panels of Fig. 8 show the original temperature profiles, while the right panels show the results after the climatological ionospheric correction, marked with a capital C.

The temperature plots (top row) show the typical behavior of low latitude profiles with a pronounced tropopause and stratopause and the influence of ionospheric errors at high altitudes. The ionospheric residual is clearly reduced after the climatological ionospheric correction (right panel), which becomes even more evident when looking at the difference plots (bottom row). These plots illustrate how the temperature errors increase with altitude and solar activity, resulting in a fan like distribution, with maximum spread at high altitudes. As an example, January 2002 has the highest $F_{10.7}$ value (226.8 sfu), see Fig. 1, and shows a maximum difference of about −3.9 K at 35 km altitude. For a solar minimum year on the other hand, as, e.g. 2008 ($F_{10.7}$ = 75.3 sfu), the temperature bias reduces to a value of −1.4 K.

Studying the corrected data sets, we find that the temperature profile of January 2002 shows a difference of about −1.0 K at 35 km altitude, while for 2008 it amounts to 0.4 K. As a result of the correction the spread of the fan is clearly reduced and even more important, it is centered around zero with maximum absolute deviations of less than about 1.0 K.

5 Summary, conclusions and outlook

For the study of neutral atmospheric parameters based on radio occultation (RO) data it is important to correct for the contribution of the ionosphere. The commonly applied linear ionospheric correction is based on the fact that the ionosphere is a dispersive medium. A combination of the two GPS frequencies leads to an ionospheric correction

AMTD
6, 1979–2008, 2013

to first order. Since this correction is an approximation, there exists an ionospheric residual, depending on the change of the solar activity. This residual results in a systematic ionospheric error, which affects the accuracy of the atmospheric parameters, also at low altitudes.

We studied this systematic ionospheric residual by analyzing the bending angle bias characteristics of CHAMP and COSMIC RO data from the years 2001 to 2011. We confirmed that the night time bending angle bias stayed constant over the whole period of 11 yr, while the day time bias increases from low to high solar activity. As a result, the difference between night and day time bias increases from about −0.05 µrad to about −0.4 µrad. This behavior paves the way to correct the solar cycle dependent bias of day time RO profiles.

As a next step we simulated RO profiles at tropical latitudes. The goal was on the one hand to study separately the influence of the ionosphere and the neutral atmosphere. On the other hand we wanted to test a first approach to reduce the ionospheric residual and the systematic error in the atmospheric parameters. First of all, our analysis showed that the contribution of the neutral atmosphere at the altitude where the bending angle bias was determined (65 km to 80 km) is small and almost constant with time. Second, by investigating retrieved dry temperature profiles, we studied the influence of the ionosphere on neutral atmosphere RO data. As expected, the influence increases with solar activity and altitude. As an example, the simulated January profiles at a latitude and longitude of 0° show a maximum bias of −3.9 K (year 2002) and a minimum bias of −1.4 K (year 2008) at 35 km altitude.

In this model world we also tried to reduce the ionospheric residual of the simulated profiles. The principle idea was to use the bending angle bias characteristics of a solar cycle (11 yr) and to correct the day time bending angle by this factor, depending on the latitude and the phase of the solar cycle. Discussing the same example as before, we found that the climatological ionospheric correction reduces the error spread at 35 km altitude from 2.5 K to 1.7 K, while the maximum absolute errors stay below about 1.0 K. These results confirm, that the proposed approach of correcting the day time bending

AMTD
6, 1979–2008, 2013

angle profiles by a solar activity dependent factor, works in principle. We note that an unknown, but apparently time constant night time bias will remain in the corrected data.

For a detailed formulation of the climatological ionospheric correction, which can be applied to observational data, it will be important to include multi-satellite RO results from the currently evolving solar maximum, since results from the last maximum are only based on RO data with comparatively high noise level from a single-satellite mission (CHAMP). A fine tuning of the applied correction will comprise a detailed study of the local time dependance of the ionospheric residual and an optimized formulation of the geographic dependance, where we will also consider if magnetic coordinates are better suited than geographic coordinates.

Another aspect, which has to be considered, is the contribution of the neutral atmosphere to the bending angle above 65 km altitude, where the bending angle bias is operationally determined in our retrieval. We have to make sure that we don't remove an apparent ionospheric bias, which is indeed a real contribution of the neutral upper atmosphere – which also shows changes caused by the solar cycle. Our preliminary analysis based on ECMWF data indicates that this effect is small and almost constant with time, but further work is needed to confirm these results. A simple approach to minimize this potential problem could be to increase the minimum altitude of the range, where the bending angle bias is determined (e.g. from currently 65 km to 70 km), which would significantly reduce any contribution from the neutral atmosphere.

Finally we want to emphasize that the goal of the proposed correction is not to improve individual profiles, but to reduce the small ionospheric residual in large ensembles of RO data for climate applications. A further advantage of the new approach is that it is model independent, based purely on observational RO data.

Acknowledgements. We are grateful to the UCAR/CDAAC and WEGC GPS RO operational team members for their contributions in OPS system development and operations. Furthermore we thank ECMWF for providing analysis data. Our work was funded by the Austrian Science Fund (FWF) under grant P22293-N21 (BENCHCLIM project). Finally we thank G. Kirchengast (WEGC) for fruitful discussions and M. Schwärz (WEGC) for his technical support.

AMTD
6, 1979–2008, 2013

References

Bassiri, S. and Hajj, G. A.: Higher-order ionospheric effects on the GPS observables and means of modeling them, Manuscr. Geod., 18, 280–289, 1993. 1982

Budden, K. W.: The Propagation of Radio Waves, Cambridge University Press, Cambridge, New York, 1985. 1982

Fjeldbo, G., Kliore, A. J., and Eshleman, V. R.: The neutral atmosphere of Venus as studied with the Mariner V radio occultation experiments, Astron. J., 76, 2, 123–140, doi:10.1086/111096, 1971. 1981

Foelsche, U., Kirchengast, G., Steiner, A. K., Kornblueh, L., Manzini, E., and Bengtsson, L.: An observing system simulation experiment for climate monitoring with GNSS radio occultation data: setup and testbed study, J. Geophys. Res., 113, D11108, doi:10.1029/2007JD009231, 2008. 1986

Foelsche, U., Scherllin-Pirscher, B., Ladstädter, F., Steiner, A. K., and Kirchengast, G.: Refractivity and temperature climate records from multiple radio occultation satellites consistent within 0.05 %, Atmos. Meas. Tech., 4, 2007–2018, doi:10.5194/amt-4-2007-2011, 2011. 1989, 1991

Fritzer, J., Kirchengast, G., and Pock, M.: End-to-End Generic Occultation Performance Simulation and Processing System Version 5.5 (EGOPS5.5) Software User Manual, University of Graz, Austria, WEGC and IGAM, WEGC–EGOPS–2009–TR01, version 1, 2009. 1986

Gobiet, A. and Kirchengast, G.: Advancements of GNSS radio occultation retrieval in the upper stratosphere for optimal climate monitoring utility, J. Geophys. Res., 109, D24110, doi:10.1029/2004JD005117, 2004. 1981

Hajj, G. A., Kursinski, E. R., Romans, L. J., Bertiger, W. I., and Leroy, S. S.: A technical description of atmospheric sounding by GPS occultation, J. Atmos. Solar-Terr. Phys., 64, 451–469, doi:10.1016/S1364-6826(01)00114-6, 2002. 1981

Hardy, K. R., Hajj, G. A., and Kursinski, E. R.: Accuracies of atmospheric profiles obtained from GPS occultations, Int. J. Satell. Commun., 12, 463–473, doi:10.1002/sat.4600120508, 1994. 1982

Ho, S.-P., Kirchengast, G., Leroy, S., Wickert, J., Mannucci, A. J., Steiner, A. K., Hunt, D., Schreiner, W., Sokolovskiy, S., Ao, C., Borsche, M., von Engeln, A., Foelsche, U., Heise, S., Iijima, B., Kuo, Y.-H., Kursinski, E. R., Pirscher, B., Ringer, M., Rocken, C., and Schmidt, T.: Estimating the uncertainty of using GPS radio occultation data for climate monitoring: in-

AMTD
6, 1979–2008, 2013

tercomparison of CHAMP refractivity climate records from 2002 to 2006 from different data centers, J. Geophys. Res., 114, D23107, doi:10.1029/2009JD011969, 2009. 1985
Hocke, K., Igarashi, K., and Tsuda, T.: High-resolution profiling of layered structures in the lower stratosphere by GPS occultation, Geophys. Res. Lett., 30, 1426, doi:10.1029/2002GL016566, 2003. 1984
Kedar, S., Hajj, G. A., Wilson, B. D., and Heflin, M. B.: The effect of the second order GPS ionospheric correction on receiver positions, Geophys. Res. Lett., 30, 1829, doi:10.1029/2003GL017639, 2003. 1983
Kuo, Y. H., Wee, T. K., Sokolovskiy, S., Rocken, C., Schreiner, W., Hunt, D., and Anthes, R. A.: Inversion and error estimation of GPS radio occultation data, J. Meteor. Soc. Jpn., 82, 507–531, 2004. 1985
Kursinski, E. R., Hajj, G. A., Schofield, J. T., Linfield, R. T., and Hardy, K. R.: Observing Earth's atmosphere with radio occultation measurements using the Global Positioning System, J. Geophys. Res., 102, 23429–23465, 1997. 1981, 1982
Ladreiter, H. P. and Kirchengast, G.: GPS/GLONASS sensing of the neutral atmosphere: model-independent correction of ionospheric influences, Radio Sci., 31, 877–891, doi:10.1029/96RS01094, 1996. 1981
Leitinger, R. and Kirchengast, G.: Easy to use global and regional models – a report on approaches used in Graz, Acta Geod. Geophys. Hung., 32, 329–342, 1997. 1986
Leitinger, R., Titheridge, J. E., Kirchengast, G., and Rothleitner, W.: A "simple" global empirical model for the F layer of the ionosphere, University Graz, Wiss. Bericht 1/1995IMG, 1995. 1986
Mannucci, A. J., Ao, C. O., Pi, X., and Iijima, B. A.: The impact of large scale ionospheric structure on radio occultation retrievals, Atmos. Meas. Tech., 4, 2837–2850, doi:10.5194/amt-4-2837-2011, 2011. 1981
Melbourne, W. G., Davis, E. S, Duncan, C. B., Hajj, G. A., Hardy, K. R., Kursinski, E. R., Meehan, T. K., Young, L. E., and Yunck, T. P.: The application of spaceborne GPS to atmospheric limb sounding and global change monitoring, JPL Publ., 94, 147 pp., 1994. 1981, 1982
Petrie, E. J., Hernández-Pajares, M., Spalla, P., Moore, P., and King, M. A.: A review of higher order ionospheric refraction effects on dual frequency GPS, Surv. Geophys., 32, 197–253, 2011. 1983

AMTD
6, 1979–2008, 2013

Pirscher, B.: Multi-satellite climatologies of fundamental atmospheric variables from radio occultation and their validation, Ph.D. thesis, Wegener Center Verlag Graz, Austria, ISBN 978-3-9502940-3-3, Sci. Rep. 33-2010, 2010. 1985
Randel, W., Chanin, M. L., and Michaut, C.: SPARC intercomparison of middle atmosphere climatologies, SPARC, WCRP 96, WMO/TD No. 1142; SPARC Report No. 3, 2002. 1988
Rocken, C., Schreiner, B., Sokolovskiy, S., Hunt, D., and Syndergaard, S.: Formosat-3/COSMIC, The Ionosphere as Signal and Noise, Space Weather Workshop, Boulder, CO, USA, 2008. 1984, 1988
Rocken, C., Schreiner, W., Sokolovskiy, S., and Hunt, D.: Ionospheric errors in COSMIC radio occultation data, paper presented at the 89th American Meteorological Society Annual Meeting, Phoenix, AZ, USA, 2009. 1984, 1988
Schreiner, B., Sokolovskiy, S., Hunt, D., Ho, B., and Kuo, B.: Use of GNSS Radio Occultation data for Climate Applications, presentation at the World Climate Research Programme (WCRP) workshop, Denver, CO, USA, 2011. 1984, 1988
Smith, E. and Weintraub, S.: The constants in the equation for atmospheric refractive index at radio frequencies, Proc. IRE, 41, 1035–1037, 1953. 1982
Steiner, A. K., Kirchengast, G., Lackner, B. C., Pirscher, B., Borsche, M., and Foelsche, U.: Atmospheric temperature change detection with GPS radio occultation 1995 to 2008, Geophys. Res. Lett., 36, L18702, doi:10.1029/2009GL039777, 2009. 1985
Sokolovskiy, S., Schreiner, W., Rocken, C., and Hunt, D.: Optimal noise filtering for the ionospheric correction of GPS radio occultation signals, J. Atmos. Ocean. Tech., 26, 1398–1403, doi:10.1175/2009JTECHA1192.1, 2009. 1981, 1989
Spilker, J. J.: Signal structure and performance characteristics, in: Global Positioning System, edited by: Janiczek, P. M., papers published in Navigation, 1, Institute of Navigation, Washington, DC, USA, Berlin, New York, 29–54, 1980. 1981, 1983
Syndergaard, S.: On the ionosphere calibration in GPS radio occultation measurements, Radio Sci., 35, 865–883, 2000. 1981, 1984
Vergados, P. and Pagiatakis, S.: Latitudinal, solar, and vertical variability of higher-order ionospheric effects on atmospheric parameter retrievals from radio occultation measurements, J. Geophys. Res., 116, A09312, doi:10.1029/2011JA016573, 2011. 1983
Vorob'ev, V. V. and Krasil'nikova, T. G.: Estimation of the accuracy of the atmospheric refractive index recovery from Doppler shift measurements at frequencies used in the NAVSTAR system, Izv. Atmos. Ocean. Phys., 29, 602–609, 1994. 1981, 1984

AMTD
6, 1979–2008, 2013

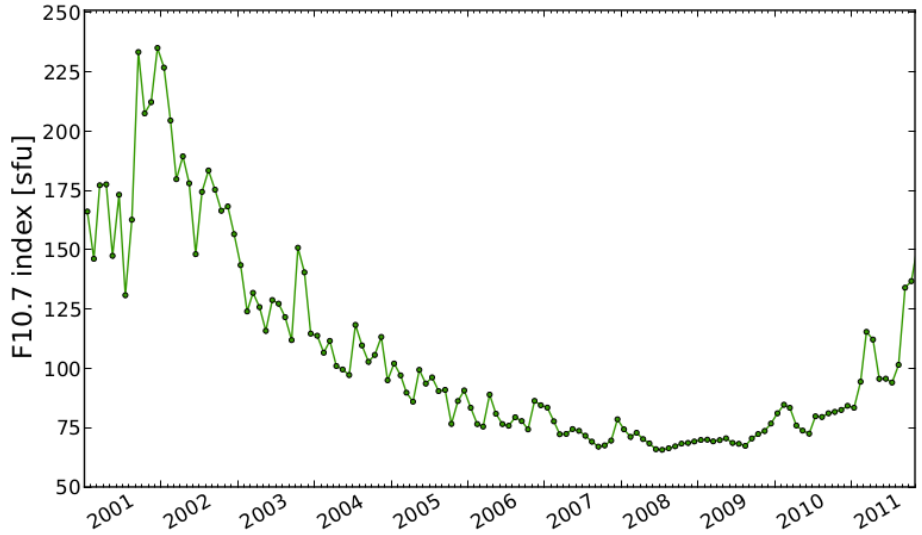

Fig. 1. Monthly mean solar radio flux ($F_{10.7}$ index) for the years 2001 to 2011 (1 sfu = $10^{-22}\,\mathrm{W\,m^{-1}\,Hz^{-1}}$).

AMTD
6, 1979–2008, 2013

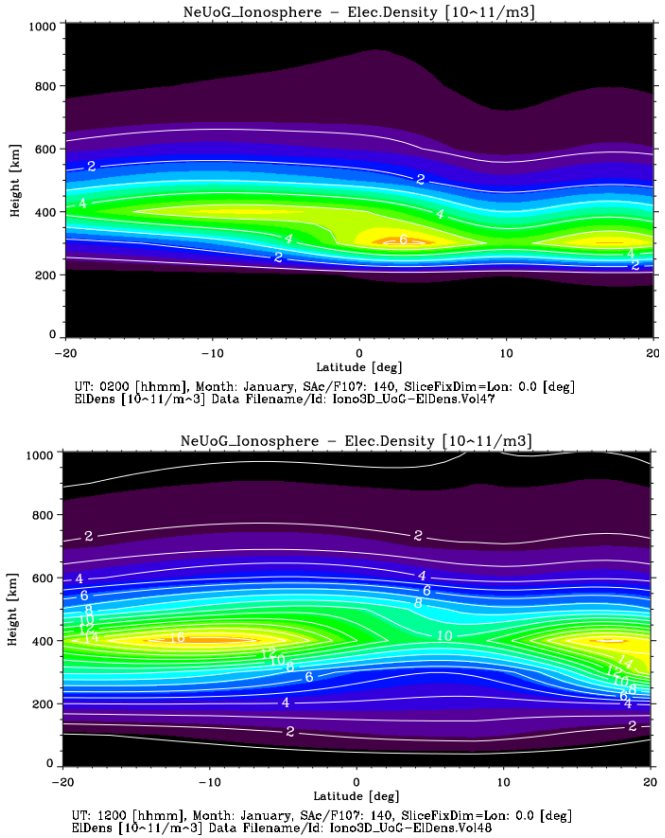

Fig. 2. Electron density distribution in January for $F_{10.7}$ = 140 sfu as a function of latitude and height, at 0° longitude. The top panel shows the distribution at night time (02:00 LT), the bottom panel shows the distribution at day time (12:00 LT), where the electron density reaches values of up to $17.5 \times 10^{11}\,m^{-3}$.

AMTD
6, 1979–2008, 2013

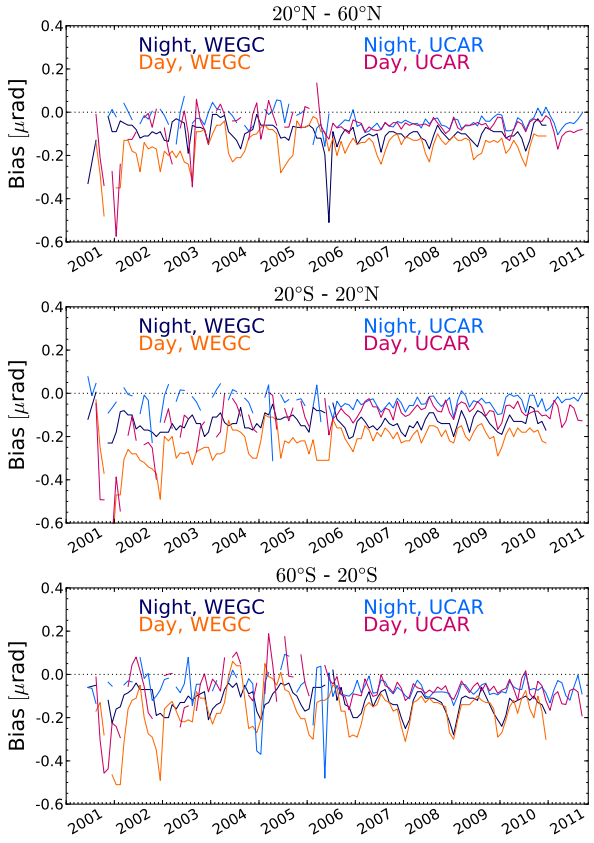

Fig. 3. Night time and day time bending angle bias characteristics over about one solar cycle for WEGC and UCAR bending angle data. From top to bottom we show data from the latitude zones 20° N to 60° N, 20° S to 20° N, and 60° S to 20° S.

AMTD
6, 1979–2008, 2013

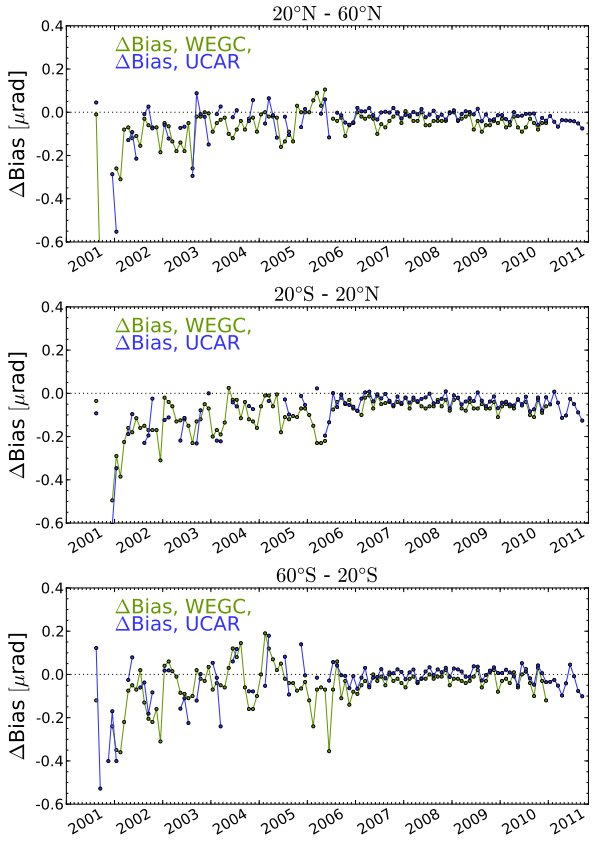

Fig. 4. Difference between day and night time bending angle bias for three latitude zones, comparing WEGC (green line) and UCAR (blue line) bending angle data (same latitude zone as in Fig. 3).

AMTD
6, 1979–2008, 2013

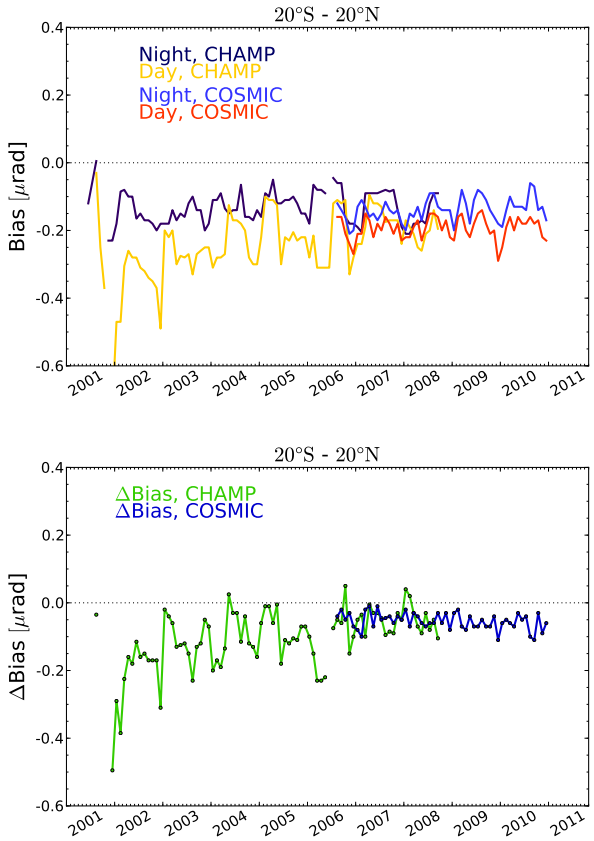

Fig. 5. Comparison of CHAMP and COSMIC bending angle bias time series based on WEGC processing. The top panel shows CHAMP and COSMIC day time and night time bias characteristics, the bottom panel displays the bias difference Δ Bias in the latitude zone 20° S and 20° N.

AMTD
6, 1979–2008, 2013

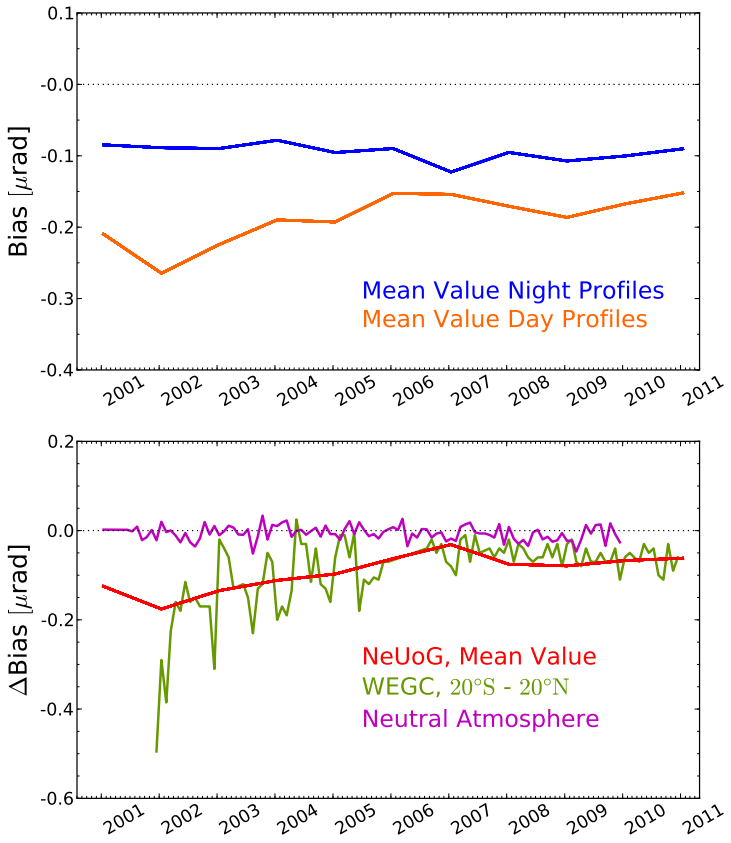

Fig. 6. Top panel: mean day time (orange line) and night time (blue line) bending angle bias of the simulated profiles. Bottom panel: mean bending angle bias difference (Δ Bias) of the simulated profiles (red line), the WEGC processed satellite data (green line) and the neutral atmosphere simulation time series at latitude and longitude 0° (magenta line).

AMTD
6, 1979–2008, 2013

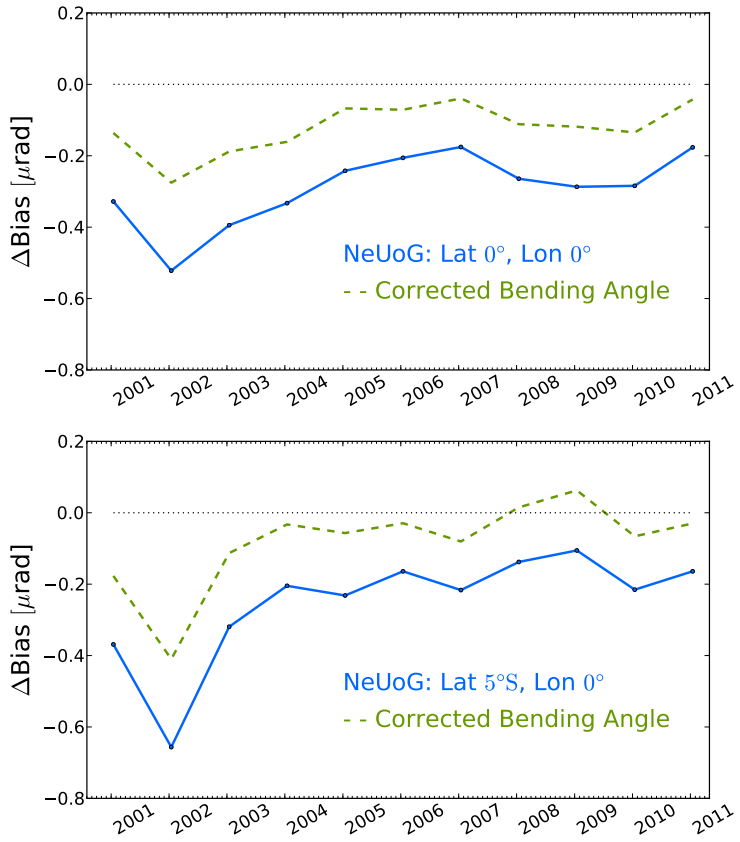

Fig. 7. Bending angle bias difference (ΔBias) between day and night for latitude 0° (top panel) and 5° S (bottom panel) for the month January from 2001 to 2011. The solid blue lines show the bending angle bias difference for original bending angle data sets, the dashed green lines show the data after climatological ionospheric correction.

AMTD
6, 1979–2008, 2013

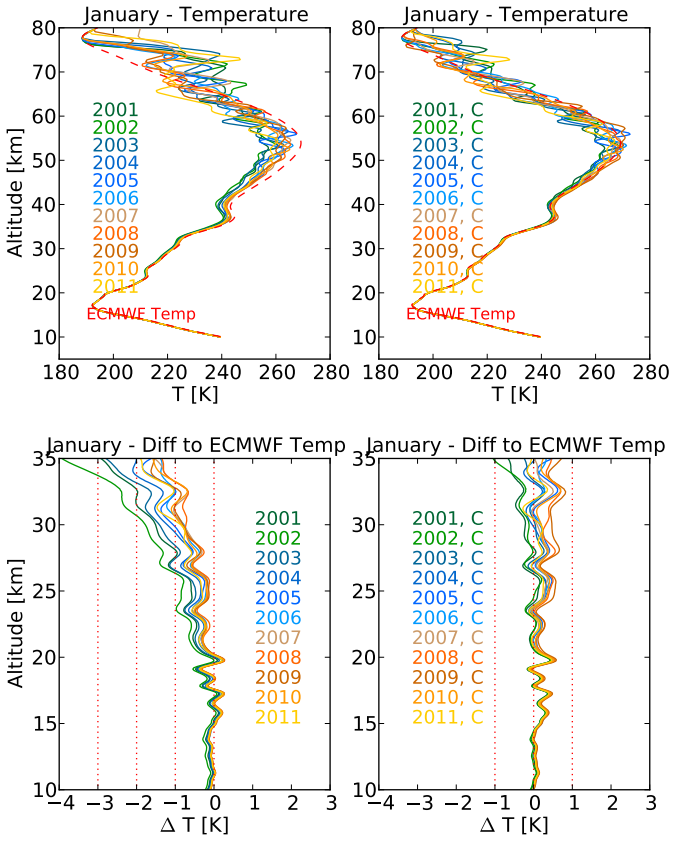

Fig. 8. Top panels: dry temperature versus altitude for January profiles from 2001 to 2011, before (left) and after (right) climatological ionospheric correction of bending angles. Bottom panels: dry temperature difference relative to the ECMWF temperature up to 35 km, again before (left) and after (right) correction. All profiles generated at latitude and longitude 0°.

AMTD
6, 1979–2008, 2013

RO residual ionospheric errors

J. Danzer et al.